1.E.1:
1.E.4:3.A

Nuclear Physics **A134** (1969) 81—109; © *North-Holland Publishing Co., Amsterdam*

LEVEL AND ISOMER SYSTEMATICS IN EVEN TIN ISOTOPES FROM ^{108}Sn TO ^{118}Sn OBSERVED IN Cd(α, xn) REACTIONS

T. YAMAZAKI † and G. T. EWAN ††

Lawrence Radiation Laboratory, University of California, Berkeley, California

Received 13 March 1969

Abstract: The gamma-ray spectra observed when separated cadmium isotopes (A = 106–116) are bombarded by 28–50 MeV α-particles from the Berkeley 2.2 m cyclotron have been studied with Ge(Li) detectors. Levels in even tin isotopes produced by (α, xn) reactions are reported. The prompt and delayed spectra have been studied using nsec time analysis and the natural beam bunching of the cyclotron to give a zero of time. Isomers have been observed in ^{118}Sn with $t_{\frac{1}{2}}$ = 20 nsec, 230 nsec and > 500 nsec, in ^{116}Sn with $t_{\frac{1}{2}}$ = 350 nsec and > 500 nsec and in ^{114}Sn with $t_{\frac{1}{2}}$ > 500 nsec and in ^{112}Sn with $t_{\frac{1}{2}}$ = 14 nsec. The level and isomer systematics in the even tin isotopes are discussed. Levels in odd tin isotopes for A = 113 to A = 119 are also discussed.

E

NUCLEAR REACTIONS $^{106, 108, 110, 112, 114, 116}$Cd($\alpha$, $xn\gamma$), ^{16}O(α, p), (α, n), (α, pn), E = 20-50 MeV; measured E_γ, $\alpha\gamma$-delay $^{107, 109, 111}$Sn deduced E_γ $^{108, 110, 112, 113, 114, 115, 116, 117, 118}$Sn deduced levels, I, π, $T_{\frac{1}{2}}$. $^{18, 19}$F, ^{19}Ne level deduced $T_{\frac{1}{2}}$. Enriched targets

1. Introduction

Isomeric states populated in nuclear reactions have been extensively studied in recent years. Usually such experiments have been performed using pulsed beams from an accelerator, and the range of lifetimes covered depended on the characteristics of the accelerator being used. Diamond, Stephens and co-workers have discovered many new isomers with half-lives 1 msec using a heavy-ion linear accelerator [1,2]). Brandi *et al.*[3]) have studied isomers with half-lives > 5 μsec produced by (γ, n) reactions using a betatron. Isomers with half-lives in the range 5–1000 μsec have been studied using pulsed beams of protons, deuterons and α-particles from cyclotrons[4–7]). Isomers in the μsec range have also been studied using a pulsed beam from a tandem accelerator [8]) In all these measurements, the half-lives have been in the μsec range or longer. It would be an obvious improvement if the range could be extended to short half-lives enabling higher-energy transitions and transitions of lower multipole order to be studied.

In recent letters [9,10]), we reported a simple method for the systematic observation of isomeric states with lifetimes longer than a few nsec populated in (particle, xn) reactions. The method depends on the natural phase grouping of beam pulses from

† Now at Department of Physics, University of Tokyo, Bunkyo-ku, Tokyo, Japan.
†† Permanent address: Chalk River Nuclear Laboratory, Chalk River, Ontario, Canada

a cyclotron and the fast timing properties of Ge(Li) detectors. We have used this method to study isomeric states in a number of Sn and Po isotopes [9,11-13]). In the present paper, we report a survey study of the level and isomer systematics of even Sn isotopes revealed in Cd(α, xn) reactions with separated cadmium isotopes.

Previously energy levels in ^{116}Sn and ^{118}Sn populated following radioactive decay have been studied by several workers [14-17]), and the levels in ^{112}Sn, ^{114}Sn and ^{116}Sn populated in (^{3}He, 3n) reactions have been studied by Betigeri and Morinaga [18]). A detailed study of the ^{116}Sn isomeric state has been performed by Chang, Hageman and Yamazaki [19]). A brief description of our results on Sn isotopes from 108 to 118 has appeared earlier [13]). In this paper, the experimental methods, the analysis of experimental data and the comparison with theoretical predictions are described in more detail.

2. Experimental method

2.1. ELECTRONIC ARRANGEMENT

In our experiments, the natural beam bunching in a cyclotron is used to give a zero of time, and the time distribution between the pulses of γ-rays from a target is studied with Ge(Li) detectors. Although this method has not previously been used for γ-ray studies, a similar technique has been used in neutron time-of-flight measurements where the neutron distribution is studied between beam pulses. Such measurements have been reviewed by Bloom [20]).

In the present experiments, the external beam from the Berkeley 2.2 m sector-focussed cyclotron has been used. The beam bunches from the cyclotron are typically 4 nsec wide, and the repetition interval is equal to the inverse of the r.f. frequency. This is in the range 100 to 170 nsec depending on the particle being accelerated and on the energy. In most of our experiments, 28–50 MeV α-particles were used to bombard the targets.

The γ-rays were studied with a Ge(Li) γ-ray detector. The fast timing properties of Ge(Li) detectors have been discussed by several workers [21,22,23]). To obtain fast timing, it is essential to use leading-edge rather than cross-over timing. This is because the pulses from Ge(Li) detectors do not have a uniform rise time. The time resolution obtainable depends on the energy of the γ-ray being studied and on the size of the Ge(Li) detector. With 3 mm thick planar detectors, FWHM of 2.7 nsec has been obtained for 511 keV γ-rays [24]). The half-slope on the edge of the curve can be as low as 1 nsec, although at $\approx \frac{1}{50}$ peak height, there is usually a tail with a greater slope.

A simplified block diagram of the present electronic arrangement is shown in fig. 1. The γ-ray signal from the Ge(Li) detector after amplification by a fast preamplifier was split into one pulse for energy analysis and another for time analysis. After further amplification by a 1 nsec fast amplifier [25]), the latter was used to trigger a fast discriminator to give a timing signal The threshold of the discriminator was set slightly above the noise level. With the planar detectors used in our experiments, this

trigger level corresponded to about 10 keV. For the large volume coaxial detectors, it corresponded to about 20 keV. The fast signal was used to generate the start signal for a time-to-height converter (EG & G Model TH200A). The stop signal was generated from the cyclotron r.f. oscillator using a fast discriminator and a suitable delay. For convenience, only every second pulse from the discriminator was used to generate a stop signal. This gives rise to two prompt peaks with a time separation of the spacing of the beam bunches as the observed γ-rays could be associated with either beam bunch. The predicted time distribution is shown schematically in the inset to fig. 1.

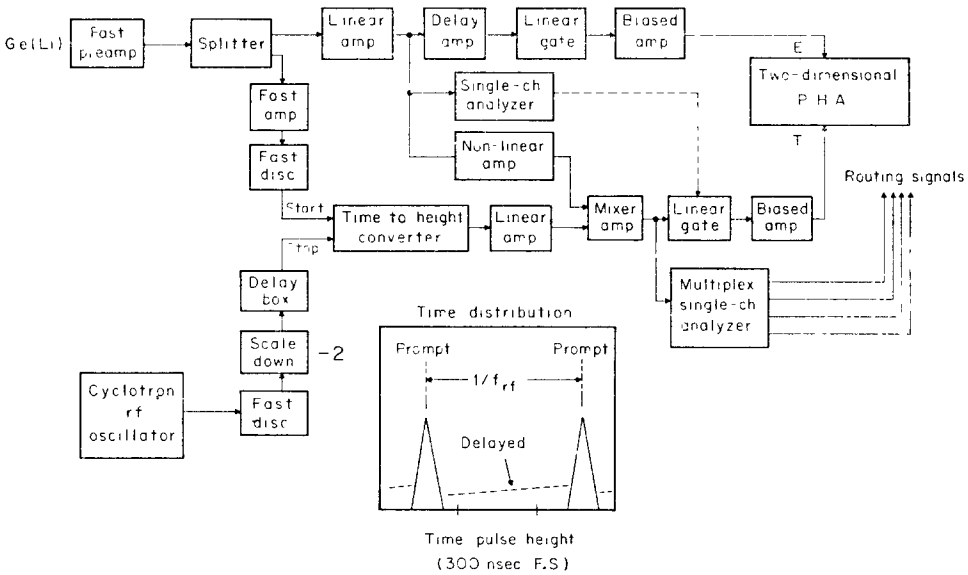

Fig. 1. Simplified block diagram of the electronic apparatus used in the present experiment. A schematic time distribution is also shown

The output of the time-to-height converter was fed to a mixer amplifier, where a correction was applied to compensate approximately for the time "walk" with pulse-height associated with leading-edge timing. This correction was not critical as we were studying time distributions of individual γ-ray peaks, and the "walk" only caused a shift in the position of "zero-time" for different energies. The energy signal from the Ge(Li) detector system and the time-signal were analysed in a two-dimensional analyser usually with 256 energy channels and 16 time channels.

2.2. EXPERIMENTAL ARRANGEMENT

A schematic diagram of the experimental arrangement used with the cyclotron is shown in fig. 2 The analysed beam struck a thin target in a simple target chamber, and the transmitted beam was stopped in a well-shielded beam catcher. The γ-ray

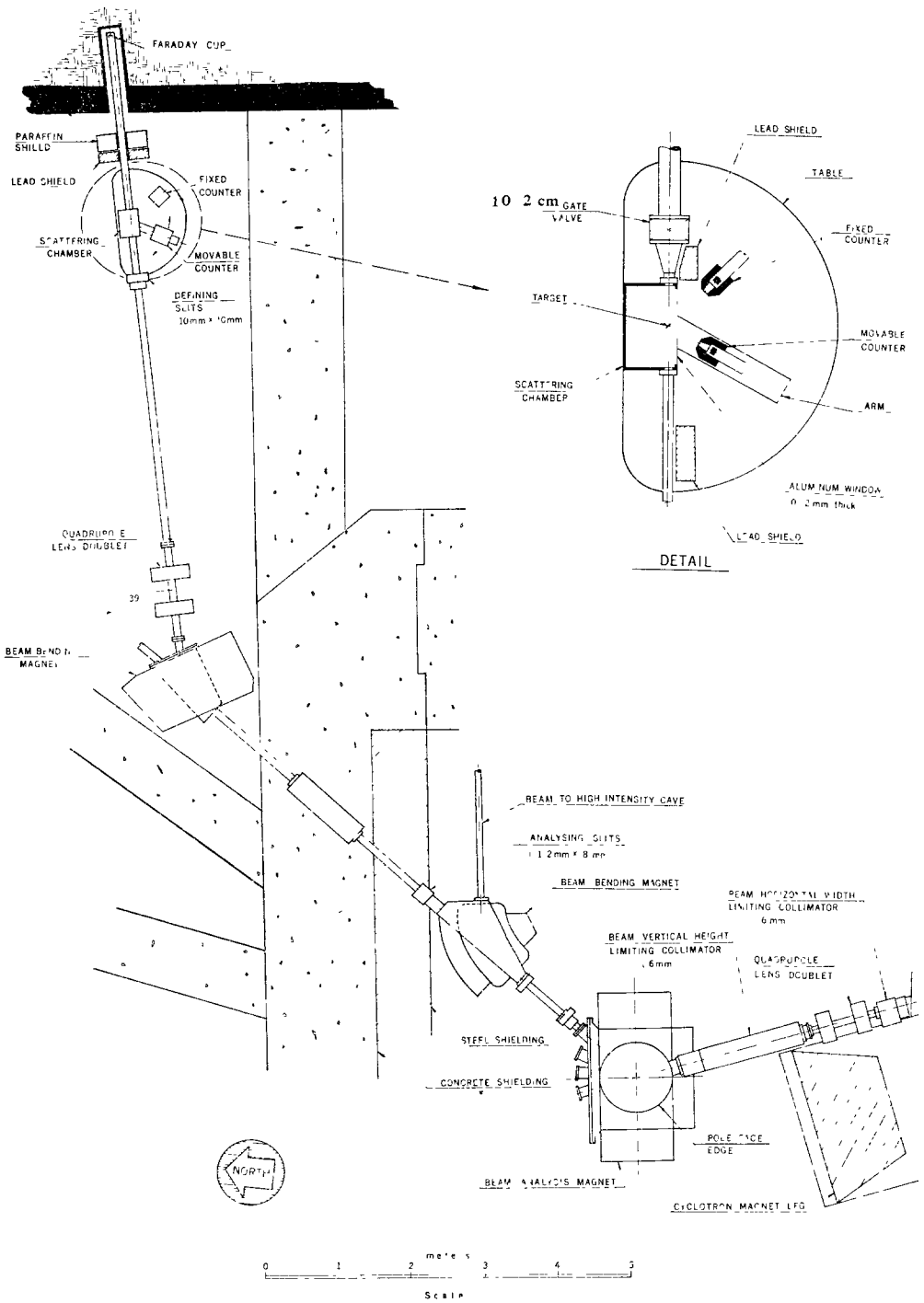

Fig. 2. Schematic diagram of the experimental arrangement used at the Berkeley 2.2 m cyclotron.

spectrum was studied with a Ge(Li) detector surrounded by a thick lead collimator to reduce the background from γ-rays from sources other than the target. In the experiments described in this paper, either a 7 $cm^2 \times 10$ mm thick planar detector or a 30 cc coaxial detector was used. The detector was usually placed at a distance of 12 cm from the target and at an angle of 126° to the beam direction in order to obtain γ-ray intensities free from angular distribution effects described by the $P_2(\cos\theta)$ term.

The Cd targets used were prepared by depositing enriched isotopes of metallic Cd on 800 $\mu g/cm^2$ thick mylar foil. The targets were typically 10–20 mg/cm^2 thick. With these thicknesses bombarded with a beam of a few nA, the background counting rate from sources other than the target was less than a few per cent of the total counting rate from the target.

2.3. EXPERIMENTAL PROCEDURE

The γ-ray spectra were initially surveyed either with 2048 channels for energy analysis and two time channels (prompt and ≈ 50 nsec delayed) or with 1024 channels for energy analysis and four time channels (prompt, 25, 50 and 75 nsec delayed). These runs immediately revealed the existence of isomers although the half-lives were not measured. The lower limit of observable half-lives in these runs was 7 nsec.

When delayed γ-rays were observed in these survey scans, a more detailed time analysis was performed. The spectra were recorded with 256 channels for energy analysis and 16 channels for time analysis. The lower limit of observable half-lives in these runs was 5 nsec. The time spacing of the cyclotron beam bunches (≈ 150 nsec) places an upper limit of 300 nsec on the measurable half-life. Longer lived isomers are easily identified but their half-lives cannot be readily determined.

The total counting rate in these runs was kept to about 3000 counts per sec and the usual counting time was approximately 30 min for each run.

2.4 BACKGROUND PEAKS IN THE γ-RAY SPECTRA

In the γ-ray spectra, there are some peaks which are due to the mylar backing of the targets, neutrons produced in the reaction and activity produced in the target Some of these peaks are present both in the prompt and delayed spectra. Some of these are identified in e.g. fig 4. The relative intensities depend on the bombarding energy.

When mylar backing is used, peaks are observed both in the prompt and delayed spectra. Mylar contains hydrogen, carbon and oxygen. The peaks in the delayed spectra are due to reactions with ^{16}O. These arise from the $^{16}O(\alpha, p)^{19}F$, $^{16}O(\alpha, n)^{19}Ne$ and $^{16}O(\alpha, pn)^{18}F$ reactions. The transitions which appear in the delayed spectra have energies of 184, 197, 238 and 939 keV. The locations of these transitions in the level schemes are shown on the right of fig. 3. The time spectra for the 197 and 238 keV γ-rays are shown on the left of fig. 3 The half-lives measured in our experiment are consistent with previous determinations [26–29]). The measured half-life of the 184 and 939 keV transition in ^{18}F was ≈ 130 nsec.

In all prompt spectra, a peak at 511 keV is observed. This is due to annihilation quanta emitted when high-energy γ-rays are absorbed by surrounding material by pair production. A peak at this energy is also usually present in the delayed spectra. This is due to the production of positon-emitting radioactive isotopes. For some heavy metallic targets such as Au and Pb used without backing material, the 511 keV γ-rays have no delayed component.

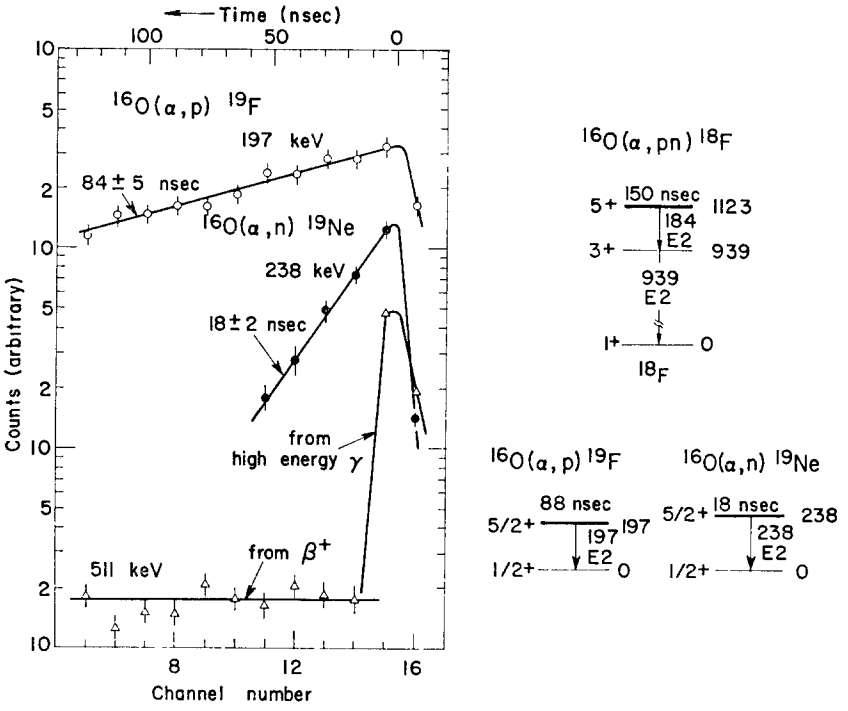

Fig. 3. Time distributions of low-energy delayed γ-rays resulting from oxygen in mylar backing of targets. The relevant level schemes are shown on the right

The broad peak around 693 keV is characteristic of all γ-ray spectra in nuclear reactions in which neutrons are produced. It is due to the (n, n') excitation of the 691 keV 0^+ excited state [30]) of ^{72}Ge in the Ge(Li) crystal. This state de-excites to the ground state and produces internal conversion electrons which are fully absorbed in the crystal. The shape of this peak is not Gaussian but skew to the high-energy side due to a contribution from the recoil of the nucleus struck by high-energy neutrons As the half-life [31]) of the 690 keV state of ^{72}Ge is 422 nsec, this peak is also seen in the delayed spectrum.

3. Experimental results

The targets and energies of bombarding particles used in our experiments are given in table 1. For these energies, the predominant reactions are (α, xn). The Q-values

TABLE 1
Targets and beams used

Target	Beam	Energy (MeV)	Predominant reaction	Residual nucleus
^{116}Cd	α	28	(α, 2n)	^{118}Sn
	α	40	(α, 3n)	^{117}Sn
^{114}Cd	α	28	(α, 2n)	^{116}Sn
	α	40	(α, 3n)	^{115}Sn
^{112}Cd	α	28	(α, 2n)	^{114}Sn
	α	40	(α, 3n)	^{113}Sn
^{110}Cd	α	28	(α, 2n)	^{112}Sn
	α	40	(α, 3n)	^{111}Sn
^{108}Cd	α	30	(α, 2n)	^{110}Sn
	α	40	(α, 2n)+(α, 3n)	^{110}Sn+^{109}Sn
	α	50	(α, 3n)	^{109}Sn
^{106}Cd	α	30	(α, 2n)	^{108}Sn
	α	40	(α, 2n)+(α, 3n)	^{108}Sn+^{107}Sn
	α	50	(α, 3n)	^{107}Sn
^{115}In	p	12, 14, 16	(p, 2n)	^{114}Sn
^{113}In	p	12, 14, 16	(p, 2n)	^{112}Sn

TABLE 2
Q-values (MeV) for Cd(α, xn) reactions

Target	(α, n)	(α, 2n)	(α, 3n)	(α, 4n)	(α, 5n)	(α, 6n)
^{116}Cd	4.3	10.8	20.1	27.0	36.6	44.1
^{114}Cd	5.3	12.2	21.8	29 3	39.6	47 4
^{112}Cd	6.2	13.7	24.0	31 8	42.9	51.8
^{110}Cd	7.7	15.4	26.5	35.4	46 6	55 9
^{108}Cd	9.3	18.2	29 4	38 7	50.3	60.2
^{106}Cd	11.1	20.4	32.1	41.9	54.1	64 5

for such reactions on the Cd isotopes used were estimated from the Myers-Swiatecki mass table [32]) and are given in table 2. For the heavier Cd isotopes, the α-particle energies of 28, 40 and 50 MeV give nearly the maximum yields of the (α, 2n), (α, 3n) and (α, 4n) reactions, respectively. For the lighter isotopes, the Q-value is greater; therefore the optimum energy should be increased correspondingly. However, for experimental convenience, we used energies of 30, 40 and 50 MeV which were below the maximum of the yield curves. It was still easy to identify γ-rays due to each reaction by comparing their yield with various targets at different beam energies. In column 3 of table 1 the predominant reaction is given and in column 4 the residual nuclei with which prominent γ-rays are associated.

In addition to (α, xn) reactions, other reactions such as (α, pxn) and (α, αxn) could also occur. Excitation functions for various α-induced reactions in this mass region were studied by Fukushima *et al.* [33,34]) by means of the activation analysis on

^{107}Ag and ^{109}Ag targets. This work confirms the assignment of prominent γ-ray peaks to (α, xn) reactions but also shows that (α, pxn) and (α, αxn) reactions are not negligible. It is difficult to identify γ-rays arising from (α, pxn) reactions. The excitation curves for these reactions are similar to that for the (α, $(x+1)$n) reaction. In our experiments, they lead to In isotopes whose level schemes are largely unknown. However, these are odd nuclei in which a large number of weak γ-rays are usually observed rather than a few strong γ-rays as is the case of even nuclei.

Since the first excited states of the Cd isotopes we used as targets are well known, it was possible to estimate the relative importance of (α, α') reactions from the yield of the γ-ray from the first excited state to the ground state of the Cd target. For the heavier targets A = 110 to 116, the contribution from (α, α') reactions was negligible. For the lighter targets A = 108 and 106, evidence was observed for γ-rays from (α, α') reactions in both the prompt and delayed spectra. Such γ-rays have a much smoother excitation curve than γ-rays from (α, xn) reactions. They will be discussed individually when considering the observed spectra for these targets.

In the cases of ^{112}Sn and ^{114}Sn, we also studied the γ-ray spectra following the In(p, xn) reaction. This provided additional data and confirmed information obtained from the Cd(α, xn) reaction. The targets and beam energies used in these studies are also listed in table 1.

3.1. THE ^{118}Sn ISOTOPE

The decay of high-spin states in ^{118}Sn has been studied by Bolotin *et al.* [14]) in studies of the radioactive decay of 5.1 h ^{118m}Sb. They established the 7^-, 5^-, 4^+, 2^+, 0^+ level sequence shown in fig. 5 and measured the half-lives of the 7^- and 5^- levels as 230 ± 10 and 20 ± 3 nsec, respectively. Ikegami and Udagawa [15]) confirmed these results.

The γ-ray spectra observed when ^{116}Cd was bombarded by 28 MeV α-particles and by 40 MeV α-particles are shown in fig. 4. The reaction at 28 MeV is predominantly (α, 2n), while the reaction at 40 MeV includes some (α, 3n) as well. In the delayed spectrum, peaks are observed at 1231.3, 1053.4, 477.9 and 254.3 keV. The time distributions of these γ-rays are shown in fig. 5. The 254, 1053 and 1231 γ-rays all have a long-lived component of $\approx 230-250$ nsec. This lifetime is too long to permit accurate measurement in the present experiments. It is attributed to population of the 230 nsec 7^- level reported from radioactive decay. The 40.7 keV γ-ray also associated with this level was below the energy range covered in our experiment. The 1053.4 and 1231.3 keV γ-rays also showed a short component of $\approx$ 20 nsec, which is ascribed to direct feeding of the 22 nsec 5^- level.

The 477.9 keV γ-ray was observed to have a long-lived component of $>$ 200 nsec as well as a prompt component. This probably is due to a level of spin $\geqq$ 8. A lower spin would permit alternative decay modes and hence a shorter lifetime. The higher spin assignment is also compatible with the relative yield of this γ-ray as a function of bombarding energy. The fact that the 477.9 keV γ-ray has a prompt component

shows that the isomeric transition must precede the 477.9 keV transition and that there is some prompt feeding of this transition as well. The isomeric transition may have too low an energy to permit observation in the present experiments (< 100 keV).

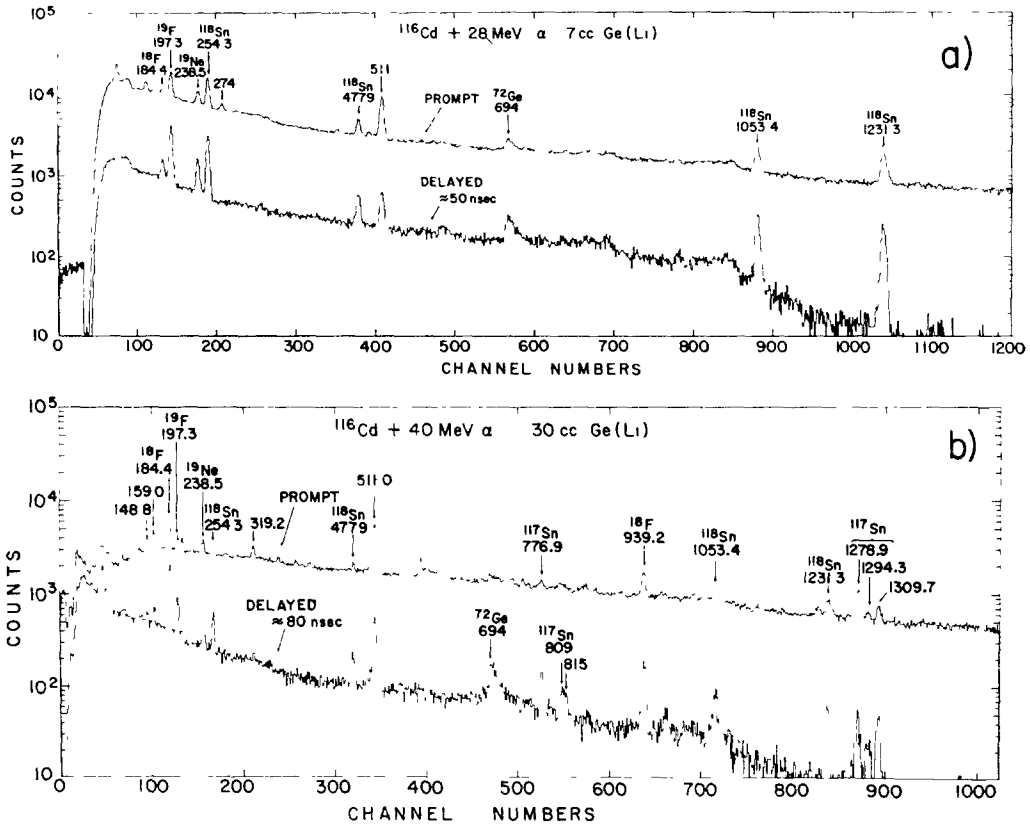

Fig. 4. Prompt and delayed γ-ray spectra observed in a) ^{116}Cd + 28 MeV α reaction and b) ^{116}Cd + 40 MeV α-reaction.

In the level scheme shown in fig. 5, the 478 keV transition is tentatively assigned as coming from an 8^+ level at 3058 keV and the isomeric transition as arising from a 10^+ level at slightly higher energy. The reasons for these tentative assignments are discussed later, when the systematics of levels in even Sn isotopes are considered.

3.2. THE ^{116}Sn ISOTOPE

Levels in ^{116}Sn have been studied [16,17]) from the radioactive decay of both ^{116}In and ^{116}Sb. The electron capture decay of 60 min ^{116}Sb populates a 7^- level at 2913 keV and lower levels as shown in fig. 7. The spin assignments to these levels are based on γ–γ angular correlation measurements and K-conversion coefficients of

γ-rays between the levels. A long-lived 5^- level was observed at 2368 keV. The half-life of this level was first [16]) measured as 200 ± 20 nsec but a later [17]) measurement gives a value of 350 ± 20 nsec.

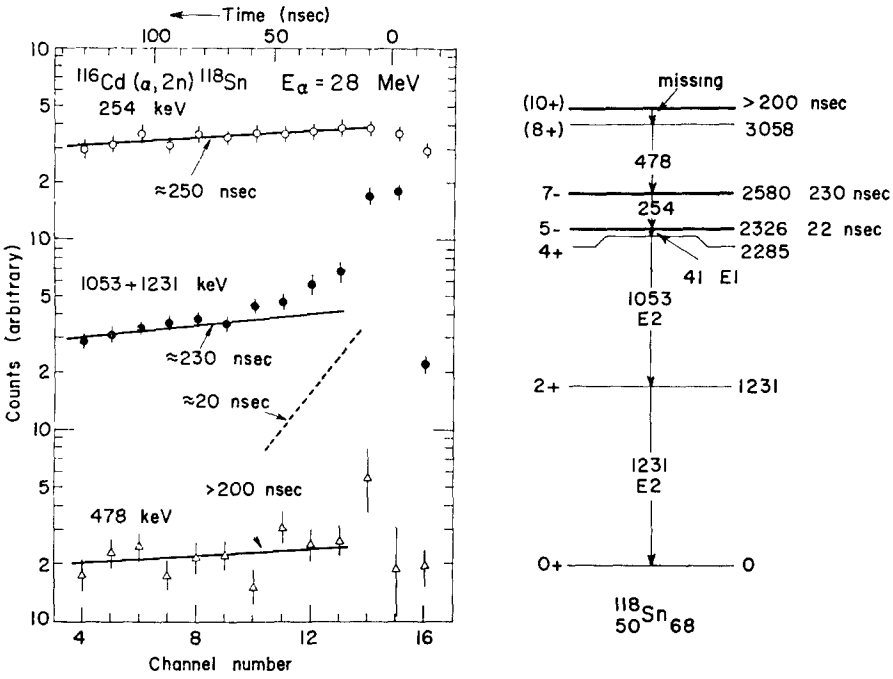

Fig. 5. Time distribution curves of ^{118}Sn γ-rays and a proposed level scheme of ^{118}Sn.

The γ-ray spectra observed when ^{114}Cd was bombarded by 28 MeV and by 40 MeV α-particles are shown in fig. 6. Many γ-rays are observed in the delayed spectrum. The time distributions of some of these γ-rays are shown in fig. 7. They all show a long-lived component (> 200 nsec), which is too long for accurate measurement in the present experiments. Chang, Hageman and Yamazaki [19]) determined the half-life of this component to be 0.75 μsec. The 100, 975, 1075 and 1293 keV γ-rays are consistent with the established decay of the 350 nsec 5^- level at 2368 keV. The 135, 408 and 544 keV γ-rays have previously been established as decay from the 7^- level at 2913 keV, whose lifetime [17]) is less than 0.2 nsec. The long-lived components must be due to feeding of this level from an isomeric state at higher energy. The 117 keV, 319 keV and 584 keV γ-rays were observed to be delayed, and the 319 and 584 keV transitions have a prompt component, thus indicating that they do not proceed directly from the isomeric state. Because of the observed intensity balance in the delayed spectrum, that is,

$$I_\gamma(319) \approx I_\gamma(135)+I_\gamma(544),$$

the 319 keV transition is readily placed on the 7^- level. The 117 keV γ-ray could be

the transition from the isomeric state, but this is questionable as no such γ-ray is observed at $E_\alpha = 20$ MeV (see the detailed study [19]) of the ^{116}Sn γ-rays). For this reason, the place for the isomeric transition is left open in fig. 7. The 319 keV transition is assigned as E1 + M2 in ref. [19]).

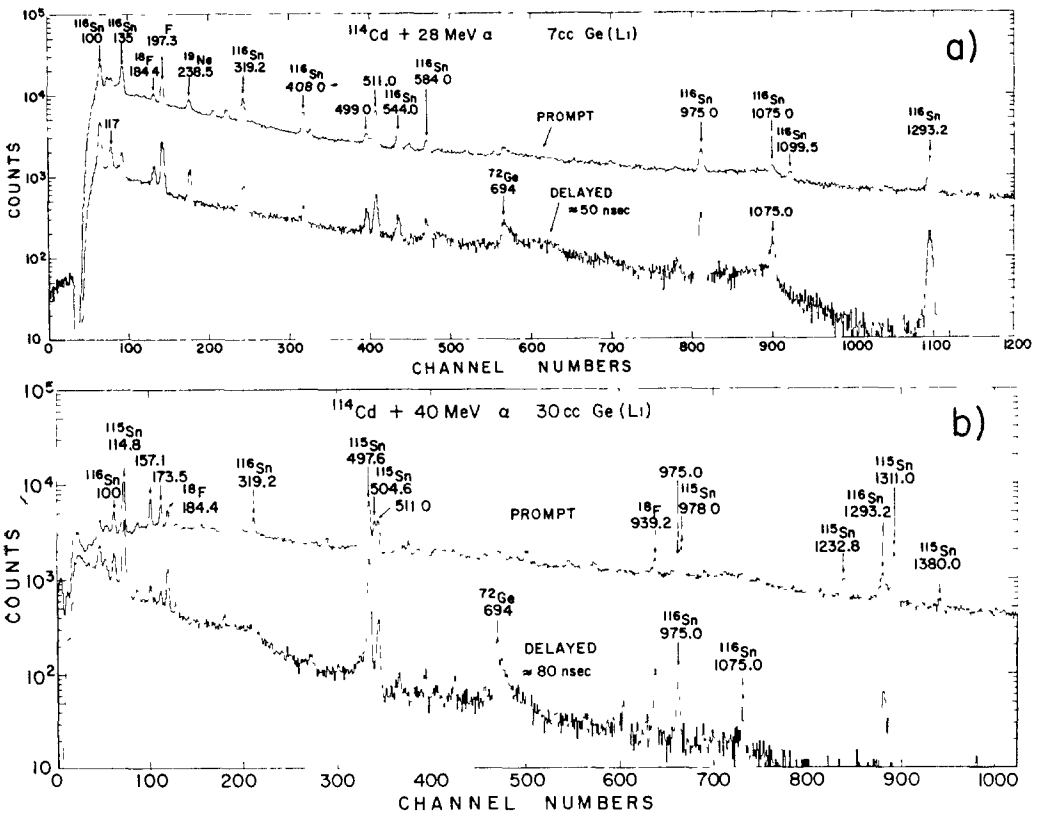

Fig. 6. Prompt and delayed γ-ray spectra observed in a) ^{114}Cd + 28 MeV α reaction and b) ^{114}Cd + 40 MeV α-reaction.

In the prompt spectrum, a 1099 keV γ-ray was observed. This was placed between the 4^+ and 2^+ states in accordance with results from the radioactive decay of ^{116}In. The population of the 4^+ state in the ^{114}Cd (α, 2n) ^{116}Sn reaction is much lower than that observed in the other nuclei. This is because higher-spin states decay to the 5^- state, which lies below the 4^+ state in ^{116}Sn. For the same reason, the transition from the 3^- to the 2^+ state was only observed in ^{116}Sn

3.3. THE ^{114}Sn ISOTOPE

Only the first excited level at 1300 keV was previously established in ^{114}Sn from studies [35]) of the radioactive decay of ^{114}Sb and ^{114}In. This level was also observed in Coulomb excitation [35]).

The γ-ray spectra observed when ^{112}Cd is bombarded by 28 MeV and by 40 MeV α-particles are shown in fig. 8. In the delayed spectra four prominent γ-rays are observed with energies 273, 628, 890 and 1299 keV. They all have equal intensities in the delayed spectra. The time distributions are shown in fig. 9. All of these γ-rays have prompt components as well as long-lived components. Their order in the level scheme was determined from the intensities of the prompt components. A 120 keV γ-ray was also observed in the delayed spectrum. No prompt component was observed, and it is assigned to a transition from the isomeric level. The half-life of the isomeric state is long ($\gtrsim$ 300 nsec).

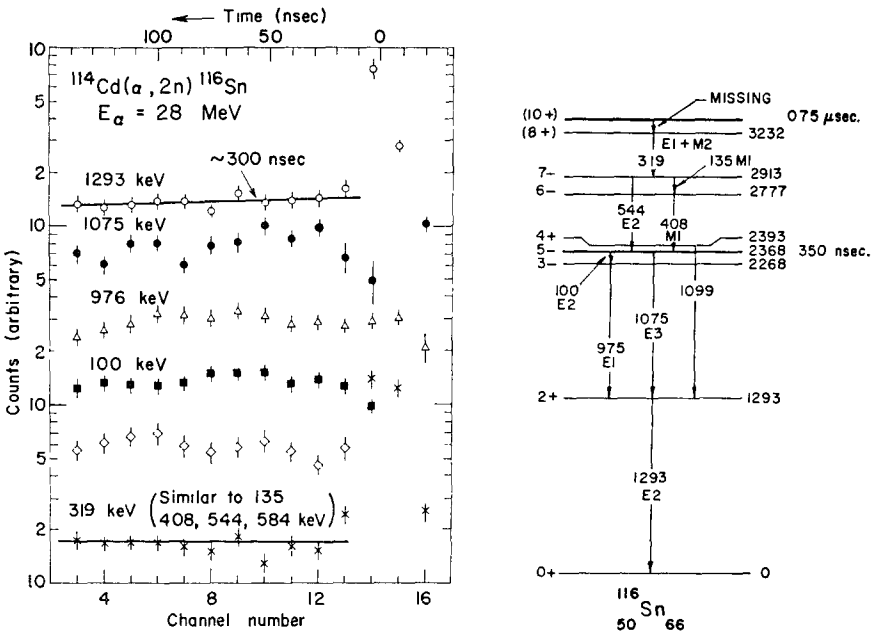

Fig. 7. Time distribution curves of ^{116}Sn γ-rays and a proposed level scheme of ^{116}Sn.

We have assigned 4^+ to the second excited state. The other possible candidate, e.g the 3^- level, is known to be located at about 2280 keV as shown in inelastic scattering experiments [36]). In the delayed spectrum, there are two weak γ-rays of 543 keV and 975 keV of equal intensity. The latter is assigned to a transition between the 3^- and the 2^+ levels and the former to a transition between the 2817 keV and the 2274 keV 3^- levels. The observation of the transitions from the 2817 keV state to both the 3^- and 4^+ states leads to the assignment of 5^- to this state.

Because very little had previously been established about the level scheme of ^{114}Sn, we also studied the γ-ray spectrum observed in the ^{115}In(p, 2n)^{114}Sn reaction at E_p = 12, 14 and 16 MeV. The γ-ray spectrum without time analysis is shown in

fig. 10. The γ-rays assigned to ^{114}Sn from the (α, 2n) reaction are all observed in this spectrum

The population of a level of given spin depends on the angular momentum transfer in the reaction. The relative yield of γ-rays is thus an indication of the spins of the levels. These yields are more sensitive in (p, 2n) reactions than in (α, 2n) reactions because of the lower excitation energy (2–5 MeV) and the lower angular momentum

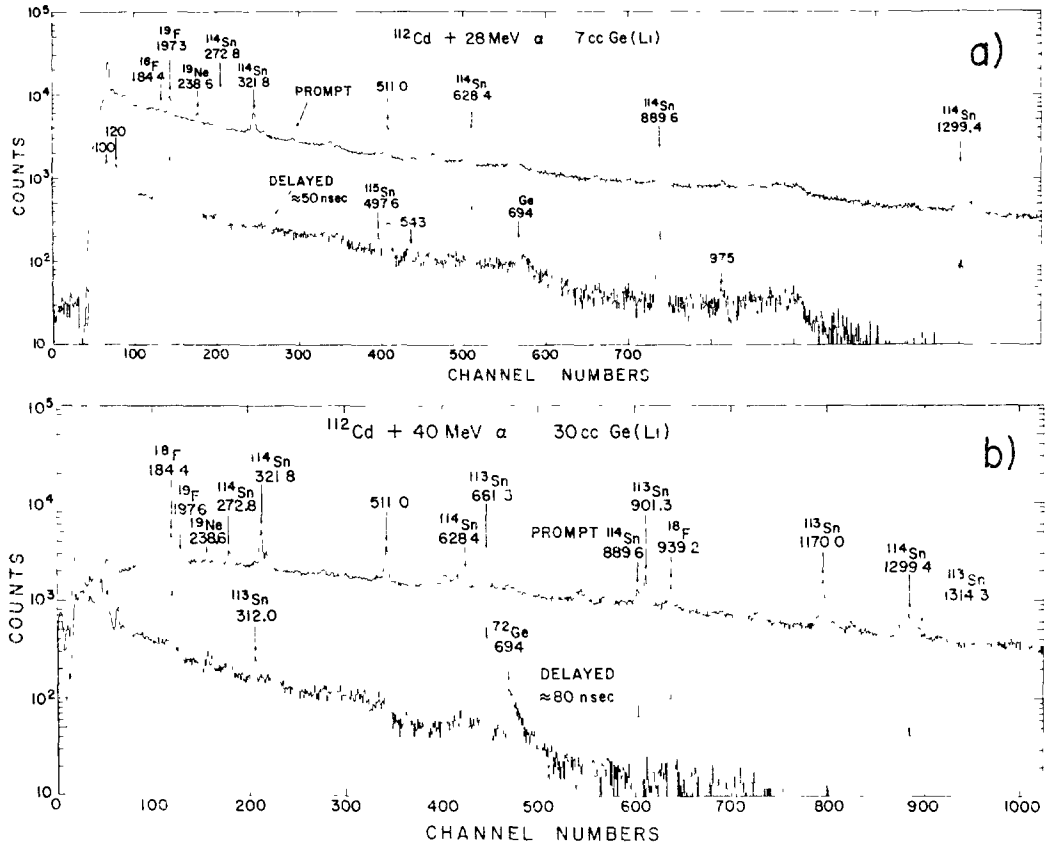

Fig 8. Prompt and delayed γ-ray spectra observed in a) ^{112}Cd + 28 MeV α reaction and b) ^{112}Cd + 40 MeV α-reaction.

transfer [37]). The variation of γ-ray intensities with energy of bombardment is shown in fig. 11. Gamma rays associated with higher-spin states show a more rapid increase with energy than the 1299 keV $2^+ \rightarrow 0^+$ transition. The results are consistent with the spin assignments given in fig. 9. The relatively higher intensity of the 975 keV transition indicates that the 3^- level is more highly populated in the (p, 2n) reaction. The relative intensities of the 543 and 628 keV transitions are independent of bombarding energy and are the same in the (p, 2n) as in the (α, 2n) reaction. This confirms the proposed assignment to γ-rays from the same level at 2817 keV.

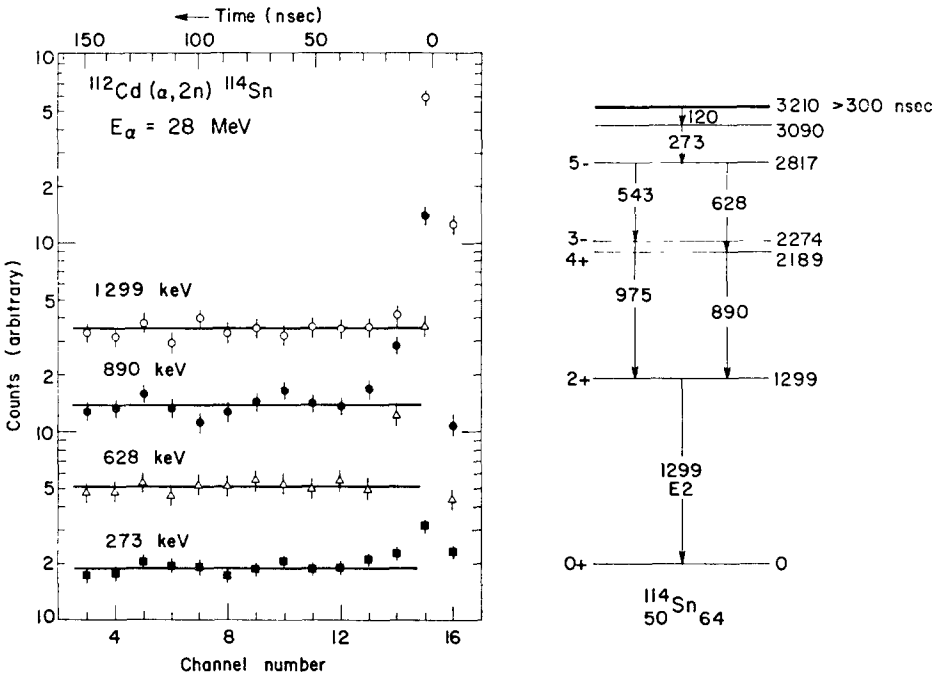

Fig. 9. Time distribution curves of ^{114}Sn γ-rays and a proposed level scheme of ^{114}Sn.

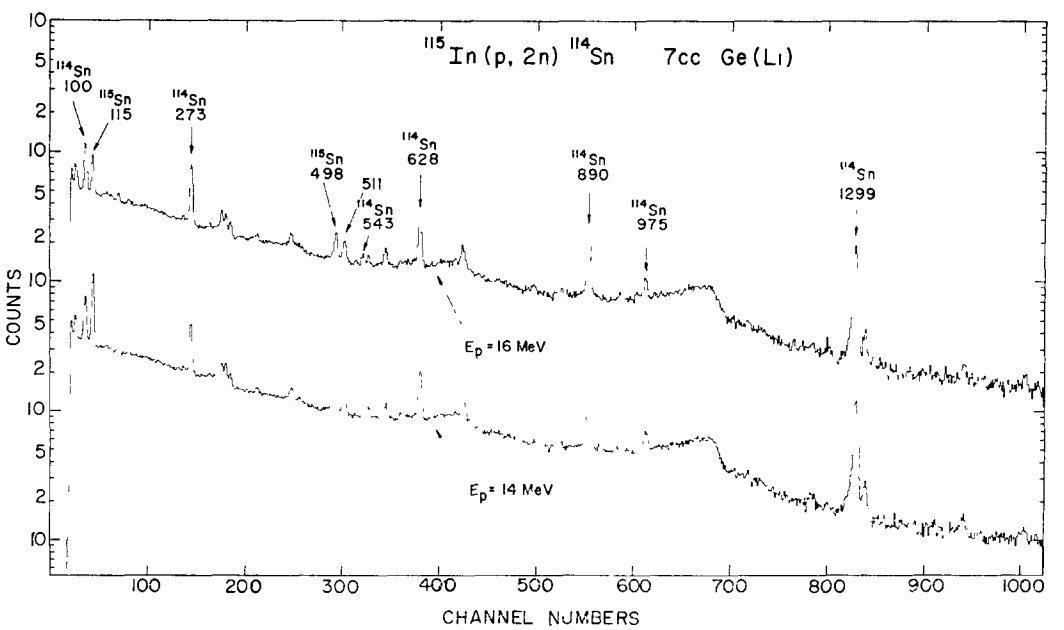

Fig. 10. Gamma-ray spectra observed when ^{115}In was bombarded with 14 and 16 MeV protons. The main reaction is ^{115}In (p, 2n) ^{114}Sn.

3.4. THE ^{112}Sn ISOTOPE

Only the first excited state was previously known [35]) from studies of radioactive decay of ^{112}Sb and from Coulomb excitation experiments. Betigeri and Morinaga [18]) observed the $2^+ \rightarrow 0^+$ γ-ray in the ^{112}Cd(^{3}He, 3n)^{112}Sn reaction.

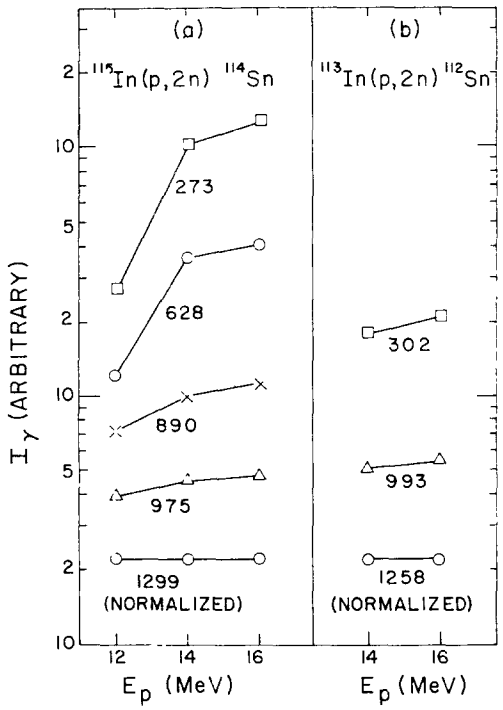

Fig. 11. Relative excitation functions of γ-rays observed when ^{115}In and ^{113}In are bombarded with protons. The γ-ray intensities given at each bombardment energy are relative to that of the $2^+ \rightarrow 0^+$ γ-ray intensity at that energy.

The γ-ray spectra observed when ^{110}Cd was bombarded by 28 MeV and by 40 MeV α-particles are shown in fig. 12. The delayed spectrum revealed three γ-rays of 302, 993 and 1258 keV of equal intensity. The time distributions of these γ-rays are shown in fig. 13. All these γ-rays have a half-life of 13.6 ± 0.6 nsec. The 1258 keV γ-ray is the most intense in the prompt spectrum and is assigned as the $2^+ \rightarrow 0^+$ transition in the level scheme in fig 13. The energy agrees with the previously known value. The 993 keV γ-ray is the next most intense in the prompt spectrum and is placed above the 1258 keV γ-ray. The 302 keV γ-ray is apparently the isomeric transition. The half-life of 14 nsec is close to the Weisskopf estimate for E2. We have tentatively assigned 4^+ and 6^+ to the 2251 and 2552 keV states, respectively. This assignment is partially based on the theoretical consideration of possible energy levels in this nucleus. The 806.6 keV γ-ray observed in the prompt spectrum is placed

above the isomeric state. The relative intensity of this γ-ray increased as the bombarding energy was increased to 40 MeV, thus indicating that it is probably a transition associated with a high-spin state at high energy.

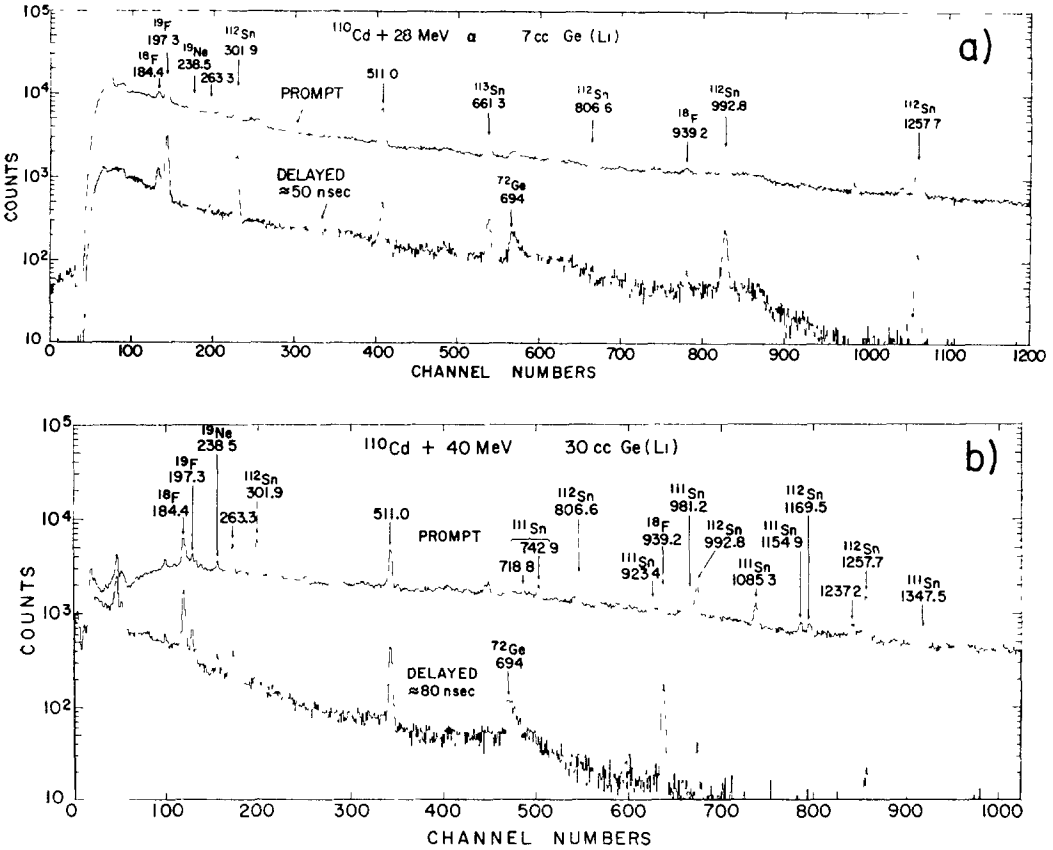

Fig. 12. Prompt and delayed γ-ray spectra observed in a) ^{110}Cd+28 MeV α-reaction and b) ^{110}Cd+40 MeV α-reaction.

The γ-rays of ^{112}Sn were also studied by the ^{113}In(p, 2n)^{112}Sn reaction. The γ-ray spectrum without time analysis is shown in fig. 14. The intensities of the observed transitions as a function of E_p shown in fig. 11 confirm the proposed order in the level scheme.

3.5. THE ^{110}Sn ISOTOPE

Nothing was known previously about the excited states of ^{110}Sn. In fig. 15, we show the γ-ray spectra observed when ^{108}Cd was bombarded by 30 MeV, 40 MeV and 50 MeV α-particles. Because of the higher Q-values, the (α, 2n) peaks appear with almost equal intensity in the spectra taken with 30 MeV and 40 MeV α-particles

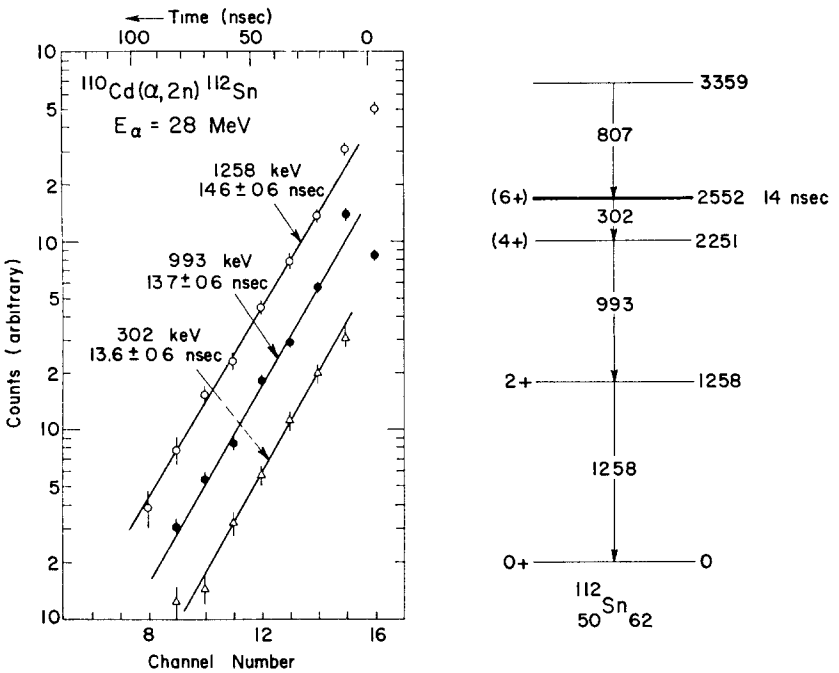

Fig. 13. Time distribution curves of ^{112}Sn γ-rays and a proposed level scheme of ^{112}Sn.

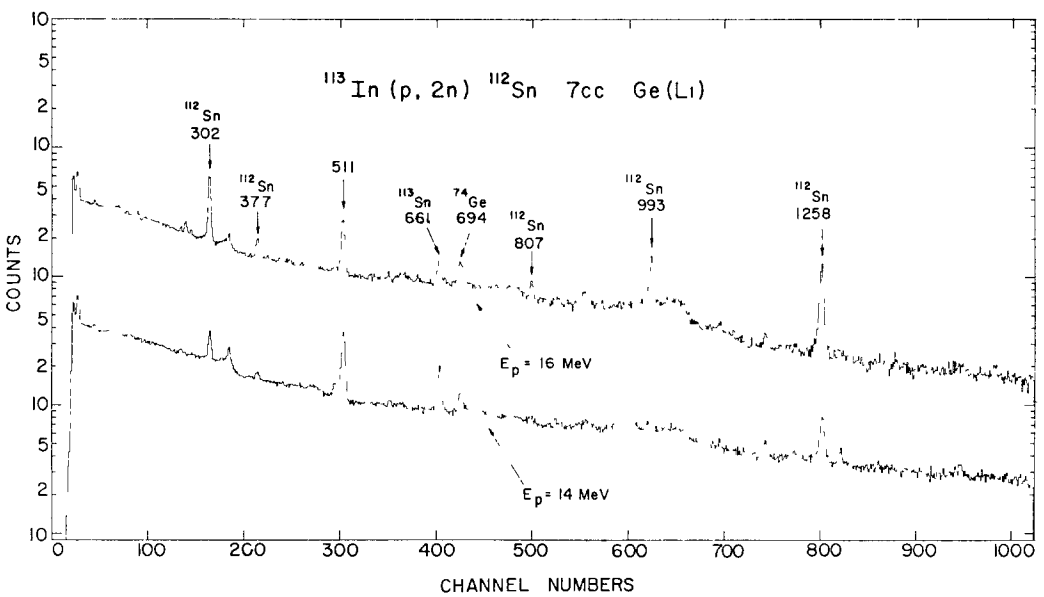

Fig. 14. Gamma-ray spectra observed when ^{113}In was bombarded with 14 and 16 MeV protons. The main reaction is ^{113}In (p, 2n) ^{112}Sn.

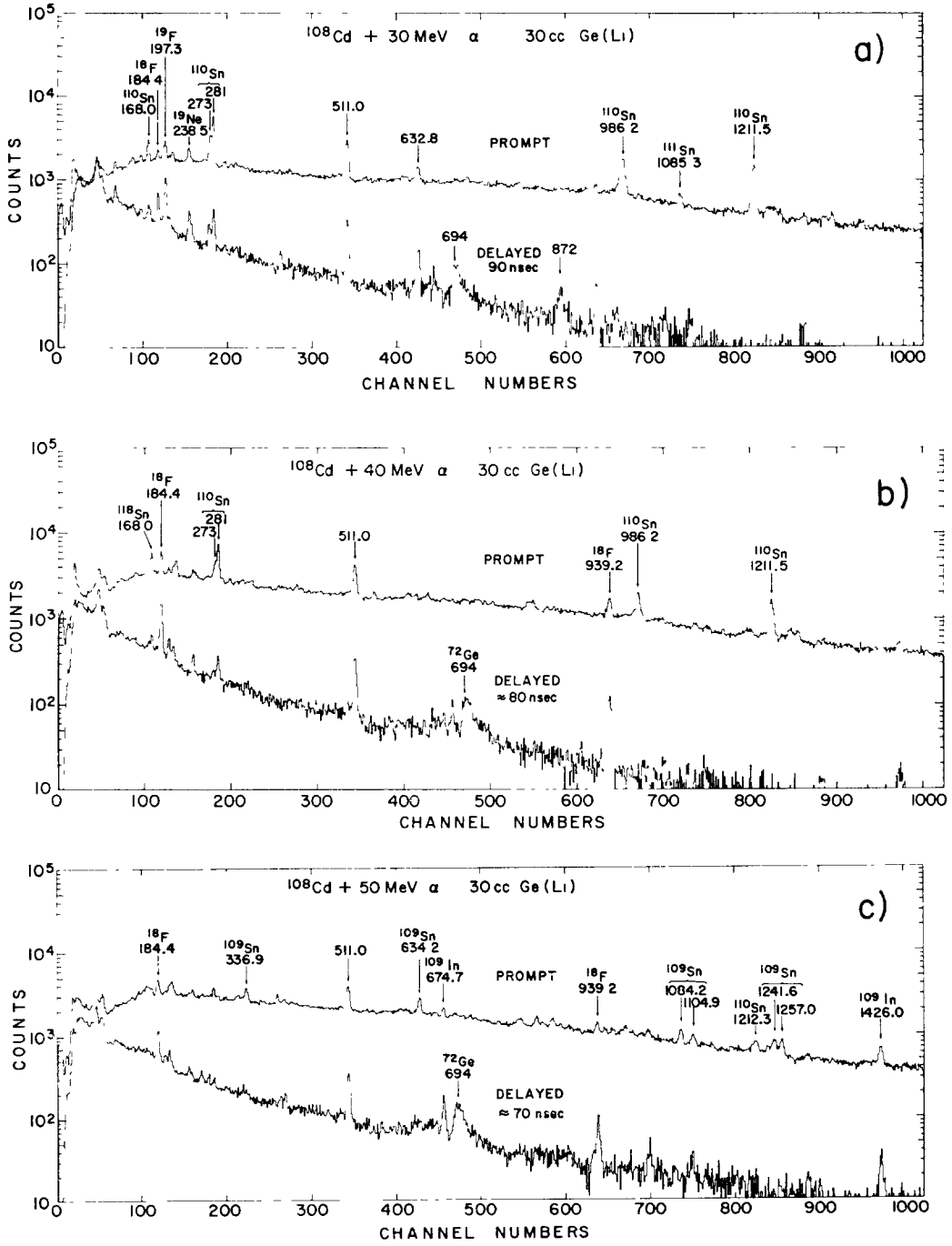

Fig. 15. Prompt and delayed γ-ray spectra observed in a) ^{108}Cd+30 MeV α-reaction, b) ^{108}Cd+40 MeV α-reaction and c) ^{108}Cd+50 MeV α-reaction.

but have almost disappeared in the spectrum taken with 50 MeV α-particles. All these spectra were taken with a large-volume coaxial detector. This had poorer timing properties than the planar detector particularly for low-energy γ-rays. As a result, the delayed spectra shows small peaks which appear to decay rapidly; this can be attributed to poor time resolution. The most prominent prompt γ-rays belonging to ^{110}Sn are 1212 keV, 987 keV and 281 keV in order of intensity. These γ-rays are placed in a level scheme shown in fig. 16b. The 1212 keV and 987 keV γ-rays show no delayed component. The 281 keV γ-ray seems to have a delayed component but this may be due to the timing properties of the detector. As we have not measured the half-life of each γ-ray, further studies are required. The half-life of the 281 keV γ-ray is certainly considerably less than that of the 238 keV γ-ray from ^{19}Ne observed in this spectrum. A limit on the half-life is less than 7 nsec.

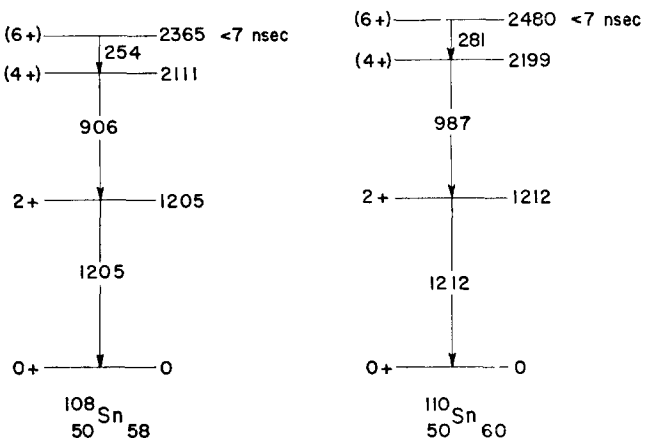

Fig. 16 Proposed level schemes of ^{108}Sn and ^{110}Sn

Weak delayed γ-rays of 633, 872 and 1098 keV are observed in fig. 15a. These γ-rays may be supposed to arise from ^{108}Cd levels through inelastic excitation for the following reasons:

(i) These γ-rays cannot belong to ^{110}Sn because of the lack of such a delayed component in the lowest $2^+ \rightarrow 0^+$ transition.

(ii) They were not seen in the ^{110}Cd + 40 MeV α-spectrum, therefore the possibility that they belong to ^{111}Sn is excluded.

(iii) The first two energies are in excellent agreement with the known energies 633 keV and 872 keV of the $2^+ \rightarrow 0^+$ and $4^+ \rightarrow 2^+$ level spacings in ^{108}Cd, respectively [35]). The half-lives of these γ-rays were not measured, but a rough estimate gives $\approx$ 100 nsec.

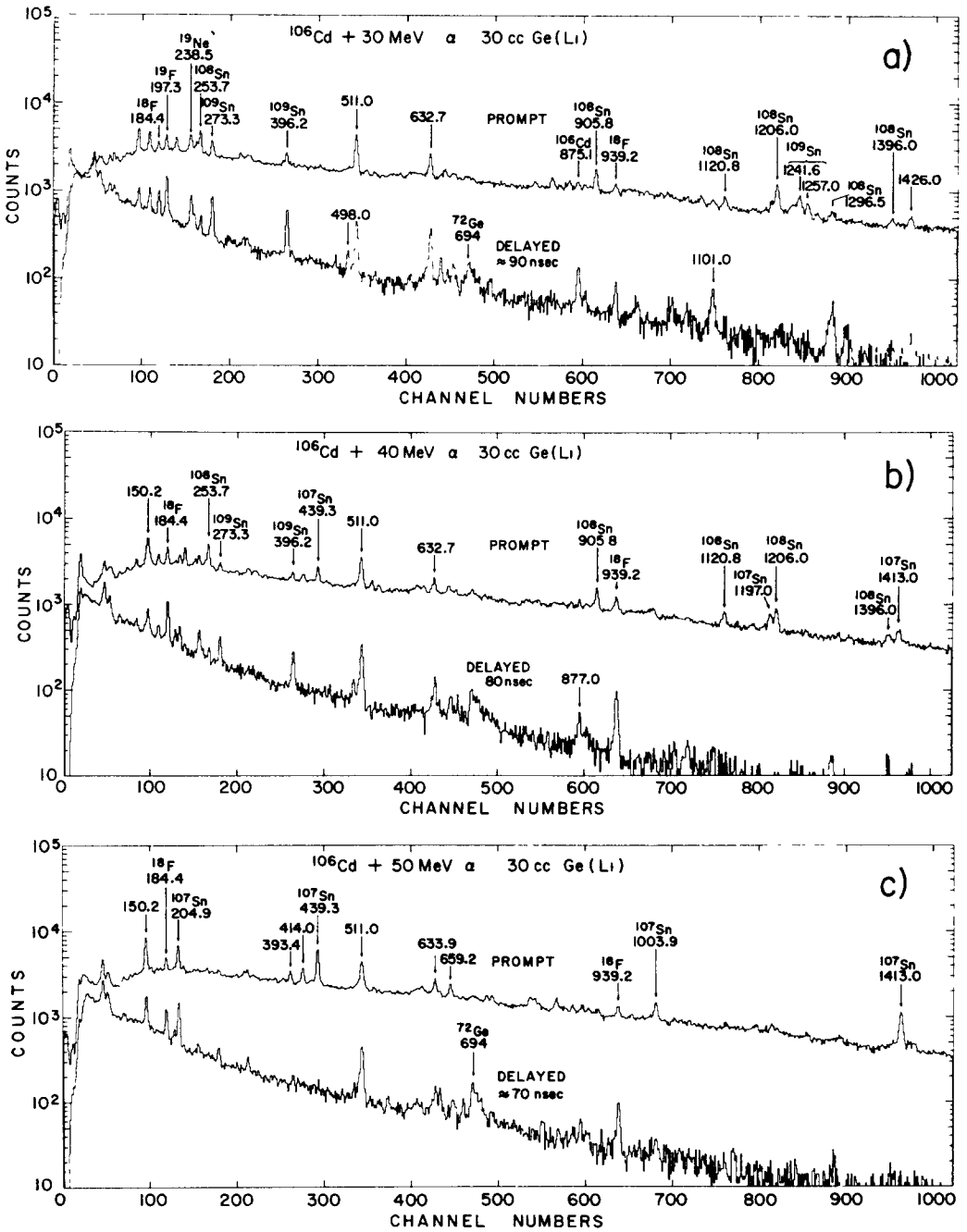

Fig. 17 Prompt and delayed γ-ray spectra observed in a) ^{106}Cd+30 MeV α-reaction, b) ^{106}Cd+40 MeV α-reaction and c) ^{106}Cd+50 MeV α-reaction.

The two delayed peaks at 675 and 1426 keV in fig. 15c were attributed to the 0.20 sec isomer [35,38]) of ^{109}In. The γ-ray energies agree with the previously known values. This isomeric state is formed in the ^{108}Cd(α, p2n)^{109}In reaction and is believed to receive a considerable part of γ-decay flow. On the other hand, the γ-decay flow in ^{109}Sn is split between many paths as shown by a number of peaks in fig 15c. The present identification indicates that the (α, p2n) yield is relatively small compared with the (α, 3n) yield even at 50 MeV incident energy. This confirms our assignment of prominent peaks to the (α, 2n) product at 30 MeV incident energy.

3 6. THE ^{108}Sn ISOTOPE

There is no previous information on any level of ^{108}Sn. The γ-ray spectra observed when ^{106}Cd was bombarded with 30 MeV, 40 MeV and 50 MeV α-particles are shown in fig. 17. The most intense 1205 keV and 906 keV peaks were identified as belonging to ^{108}Sn These γ-rays have no delayed component. The 253 7 keV γ-ray is the next most intense γ-ray. These three γ-rays are placed in a level scheme shown in fig. 16a.

Two delayed γ-rays of 633 and 875 keV might be attributed to ^{106}Cd for similar reasons to those given in subsect. 3.5.

3.7 ODD Sn NUCLEI

Prompt and delayed γ-rays belonging to odd Sn nuclei were observed in the spectra at $E_\alpha = 40$ MeV. However, the construction of level schemes is very difficult because of many possible γ-decay branches. In fig. 18, we show tentative level schemes indicating the presence of isomeric states in ^{117}Sn, ^{115}Sn and ^{113}Sn

The first four levels in ^{117}Sn are previously known. However none of the observed γ-rays in our delayed spectra corresponds to transitions between these levels. The 777 keV, 1310 keV and 1279 keV γ-rays are equally intense in the delayed spectra, but the prompt intensities increase in the above order These transitions are considered to be in cascade as shown in the figure. They are placed above the $\frac{11}{2}^-$ level, as no evidence was observed for the $\frac{3}{2}^+ \rightarrow \frac{1}{2}^+$ transitions.

The 159 μsec isomeric state of ^{115}Sn was identified at 726 keV by Ivanov *et al.* [39]) with the ^{115}In(p, n)^{115}Sn reaction From a detailed coincidence study, they concluded that the 117 keV peak consists of two transitions at 107 keV (M2) and 120 keV (E2) in cascade. The total conversion coefficients they determined were 5.4 and 0.78, respectively. The γ-ray intensity ratio is 1 : 4. In the delayed spectrum in fig. 6b, the 114 8 keV and 497.6 keV γ-rays originating from this isomer are observed, but the doublet peak is not resolved Therefore, it is assumed in the present level scheme that both γ-rays have almost the same energy of 115 keV. Recently Ivanov and Magda (ref. [40])) determined the half-life of the 619 keV state to be 3 26±0 08 μsec. The (d, p) experiment by Schneid, Prakash and Cohen [41]) revealed the presence of the $\frac{1}{2}^+$, $\frac{3}{2}^+$, $\frac{7}{2}^+$ and $\frac{11}{2}^-$ one-quasiparticle states of energies as indicated in fig 18.

In fig 8b, a new delayed γ-ray of 661.2 keV is assigned to ^{113}Sn This energy is in

good agreement with the spacing between the $\frac{11}{2}^-$ and $\frac{7}{2}^+$ levels revealed in the (d, p) experiment [41]). This would be an M2 transition similar to the 159 μsec M2 transition in ^{115}Sn. The half-life was not measured. Allowing for the difference in energy, it would be $\approx$ 20 nsec if similar to the 159 μsec isomer state in ^{115}Sn. Another delayed peak at 312 keV is also seen in fig. 8b, but as it is weak, its assignment to ^{113}Sn is suspect. There is no delayed γ-ray identified in odd nuclei lighter than ^{113}Sn.

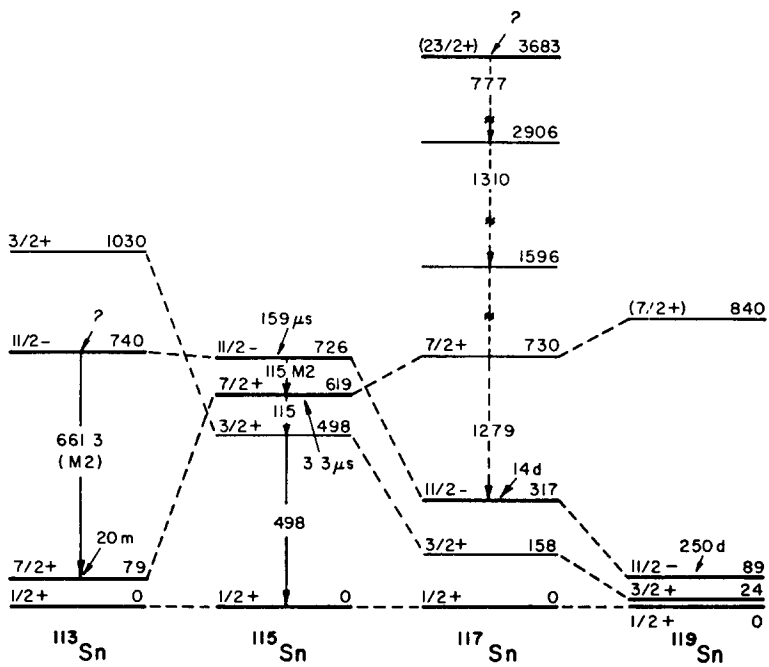

Fig 18 The isomer systematics of odd Sn isotopes. The present study has revealed a highly excited isomer of ^{117}Sn and a 740 keV $\frac{11}{2}^-$ isomer of ^{113}Sn.

4. Discussions of the level and isomer systematics

The Sn isotopes are single-closed-shell nuclei in which 50 protons constitute an inert closed shell. The properties of such nuclei have been studied extensively with the microscopic theories of nuclear structure since the first BCS calculation of Kisslinger and Sorensen [42]). Arvieu and co-workers [43,44]) performed detailed calculations using the pairing scheme and a Gaussian-type residual interaction. Plastino, Arvieu and Moszkowski [45]) used a surface delta interaction (SDI). These calculations involve only excitation up to two-quasiparticle (seniority 2) and are termed the quasiparticle Tamm-Dancoff method (QTD). Recently Ottaviani *et al.* performed calculations including four-quasiparticle (seniority 4) excitation with short-range residual interactions [46]) and also with Gaussian and Q–Q interactions [47]). More recently,

Gmitro *et al.* [48]) performed similar calculations with realistic forces. They showed that it is important to project out spurious states due to the number non-conservation introduced by the Bogoliubov transformation, and that the 0^+ and 4^+ states involve appreciable four-quasiparticle components. These calculations are called the quasiparticle second Tamm-Dancoff method (QSTD).

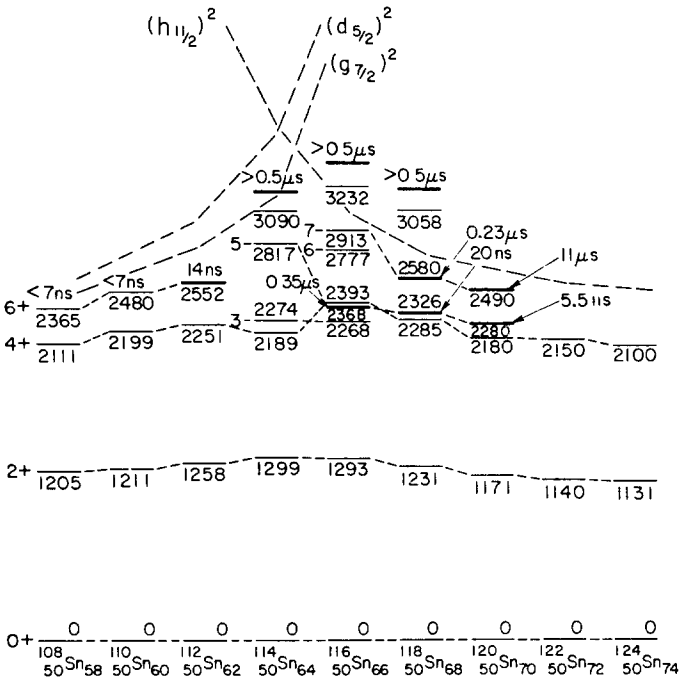

Fig. 19. The level and isomer systematics revealed in the present study. Levels of the same spin and parity are connected by broken lines. Previously known levels given in the compilation of Lederer *et al.* [35]) are included

Calculated level energies depend on the parameters chosen for the forces, and comparison of experimental level energies with the calculations may not be a critical test of a theory if only applied to one or two isotopes. As a result of the present and earlier work, information is now available on a large range of even Sn nuclei from $A = 108$ to $A = 124$. These have a closed proton shell $Z = 50$ and values of N from 58 to 74. The single-particle neutron orbits in the $d_{\frac{5}{2}}$ and $g_{\frac{7}{2}}$ orbitals and the second in the $N = 50$–82 region are grouped into two regions; the first has neutrons in the $s_{\frac{1}{2}}$, $d_{\frac{3}{2}}$ and $h_{\frac{11}{2}}$ orbitals. These two regions are divided by a soft closed sub-shell at $N = 64$. Comparison of theoretical predictions over this large range of isotopes is a good test of the validity of the theory.

The level systematics revealed in the present work cover the region below the sub-shell boundary at $N = 64$ and the boundary region. Earlier results are available on

the heavier region. The level and isomer systematics are summarized in fig. 19. We shall make some qualitative comparisons of these levels with theoretical predictions.

Quasiparticle energies calculated and used by Arvieu [44]) are illustrated in fig. 20 as functions of mass number. It is apparent that the $d_{\frac{5}{2}}$ and $g_{\frac{7}{2}}$ orbits dominate the lighter isotopes ($A < 114$), while the $s_{\frac{1}{2}}$, $d_{\frac{3}{2}}$ and $h_{\frac{11}{2}}$ orbits dominate the heavier isotopes ($A > 114$).

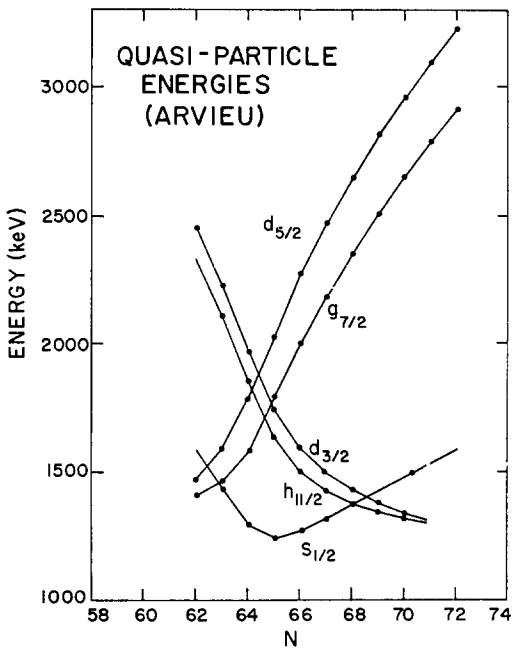

Fig. 20. Neutron quasiparticle energies calculated and used by Arvieu [44]).

4.1. FIRST 2^+ STATES

The experimental level energies are plotted in fig. 21. It is seen that the energy increases with N from $N = 58$ to $N = 64$, where it reaches a maximum, and then starts to decrease. This fact seems to reflect a slight shell effect at $N = 64$. The QTD calculations of Arvieu *et al.* [43, 44]) gave somewhat higher energies and a more distinct maximum at $N = 64$ as shown in fig. 21. The QSTD calculations of Ottaviani *et al.* [47]) with a finite-range force was performed for $A = 116$, 120 and 124, and their results are shown in the same figure.

4.2. FIRST 4^+ STATES

The experimental level energies are plotted in fig. 22. The energy of the first 4^+ level shows a dependence on N similar to that of the 2^+ level energy except at $N = 64$, where there is an appreciable depression of energy. The calculations of Arvieu *et al.* [43, 44]) is shown in fig. 22 with predominant two-quasiparticle components in the

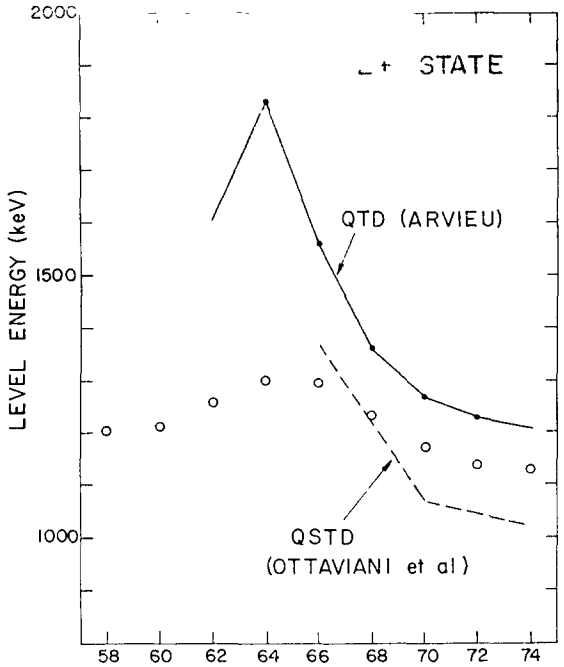

Fig 21. Comparison of the experimental energies of the first 2^+ states shown as open circles, with the QTD calculation by Arvieu *et al* [43,44]) and the QSTD calculation by Ottaviani *et al.* [47])

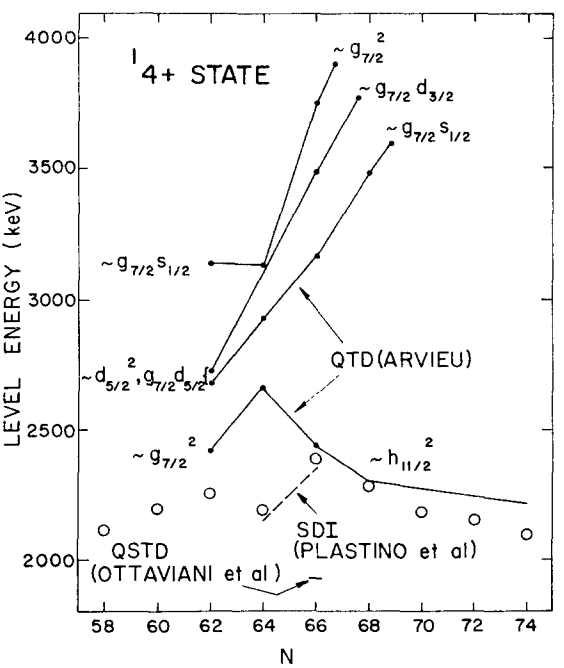

Fig 22. Comparison of the experimental energies of the first 4^+ states shown as open circles, with the QTD calculations by Arvieu *et al.* [43,44]), the SDI calculation by Plastino *et al* [45]) and the QSTD calculation by Ottaviani *et al.* [47]) The main two-quasiparticle configurations are shown for the four 4^+ states calculated by Arvieu *et al.* [43,44])

two regions. The energy dip at $N = 64$ is not reproduced in the calculations of Arvieu *et al.*, but a qualitative understanding of the dip may be obtained by considering the structure of the first 4^+ state. Below $N = 64$, its structure is dominated by the $(d_{\frac{5}{2}})^2$, $(g_{\frac{7}{2}})^2$ and $d_{\frac{5}{2}} g_{\frac{7}{2}}$ components and above $N = 64$ by the $(h_{\frac{11}{2}})^2$ component. At $N = 64$, all components contribute approximately equally and lead to a lowering in the energy of the state. The first 2^+ state is less affected because more configurations are available. It is interesting that the SDI calculations of Plastino, Arvieu and Moszkowski [45]) reproduced the experimental behaviour at $N = 64$ and 66 (see broken lines in fig. 22). The QSTD calculations with a finite-range force yielded a lower $^1 4^+$ energy because of four-quasiparticle components, but this has been performed only for $N = 66$.

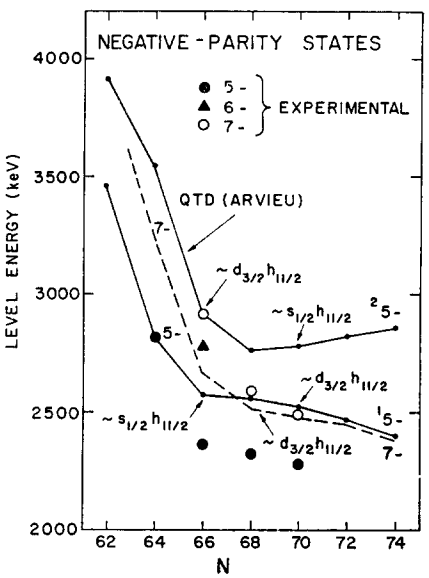

Fig. 23. Comparison of the experimental energies of the negative-parity states with the calculation of Arvieu *et al* [43, 44]). The main-two-quasiparticle configurations are shown.

4.3. NEGATIVE-PARITY STATES

The experimental levels are presented in fig. 23 with Arvieu's energies. The 5^- state ($s_{\frac{1}{2}} h_{\frac{11}{2}}$ and/or $d_{\frac{3}{2}} h_{\frac{11}{2}}$) is isomeric for $A = 116$, 118 and 120 but not for $A = 114$, where the energy difference between the 5^- and the 4^+ levels is too great for the E1 transition to have a lifetime measurable in our experiments. The 7^- state (predominantly $d_{\frac{3}{2}} h_{\frac{11}{2}}$) is isomeric for $A = 118$ and 120 due to the highly hindered E2 decay but not for $A \leqq 116$ as it feeds the 6^- state via a fast M1 transition. The 7^- level for $A = 114$ could not be identified, presumably because it lay too high for observation. The systematics of these negative-parity states are consistent with the expected behaviour of the $h_{\frac{11}{2}}$ orbit.

4.4. ISOMERIC STATES ABOVE THE 7⁻ STATES

In addition to the negative-parity isomers, at least one long-lived isomer ($\gtrsim$ 0.2 μsec) has identified for each isotope in the region $N \geqq 64$. On the other hand, no such isomer was seen in the region $N < 64$. The half-life of the isomer in ^{116}Sn has been determined by Chang, Hageman and Yamazaki [19]) to be 0.75 μsec.

This fact may be explained by the following conjecture. From the quasiparticle states available, these long-lived isomers are tentatively assigned to the 10^+ state of the $h_{\frac{11}{2}}^2$ configuration. For $N \geqq 64$, the 8^+ and 10^+ states of the $h_{\frac{11}{2}}^2$ configuration are expected to lie around 3 MeV and, as no other configuration of seniority 2 contributes to these high-spin states, they should remain relatively unperturbed. The energy spacing between the 8^+ and 10^+ levels is estimated to be about 100 keV, and the 10^+ state could be expected to have a half-life of about 1 μsec. The conjectured isomeric E2 transitions were not observed in the present survey, and further experiments are required to establish their existence. In the region $N < 64$, the $h_{\frac{11}{2}}^2$ energy becomes so large that this configuration may no longer be the sole contributor to the 8^+ and 10^+ states. Four-quasiparticle states and vibrational states may also contribute. This may explain why the long-lived isomer does not exist in this region.

TABLE 3

Experimental B(E2, $6^+ \rightarrow 4^+$) values for ^{108}Sn, ^{110}Sn and ^{112}Sn

A	E_γ (keV)	$T_{\frac{1}{2}}$ (nsec)	B(E2, $6^+ \rightarrow 4^+$) (e^2 fm^4)	B(E2)/B(E2)$_W$
112	302	14	16.3	0.25
110	281	< 7	> 46	> 0.7
108	254	< 7	> 77	> 1.2

4.5. THE 6^+ STATES FOR $N < 64$ AND B(E2, $6^+ \rightarrow 4^+$)

It is interesting that for $N < 64$ the highly populated levels terminate at 6^+. This is consistent with the fact that no higher-spin state is available at low energy with the $d_{\frac{5}{2}}$ and $g_{\frac{7}{2}}$ orbits

The half-life of the 6^+ state in ^{112}Sn was found to be 14 nsec, which is comparable with the Weisskopf estimate for an E2 transition. It is striking that no delayed state was observed for the lighter nuclei, although the level structure is unchanged. The B(E2, $6^+ \rightarrow 4^+$) values deduced from these experimental data are shown in table 3. The B(E2) value increases rapidly as N decreases This seems to be in disagreement with a simple pairing theory which predicts that the B(E2, $6^+ \rightarrow 4^+$) value should decrease due to the $(UU-VV)^2$ factor. This point has, however, to be examined with a more extensive calculation which takes into account possible configuration mixing and coupling with the collective mode.

4.6. POSSIBLE THREE-QUASIPARTICLE ISOMER IN ^{117}Sn

The present study revealed the presence of a highly excited isomeric state in ^{117}Sn with energy $\approx$ 3.68 MeV. No such isomer was found in other nuclei where only

the single-particle states and the low-lying isomeric state ($h_{\frac{11}{2}}$ state) are present The isomeric state in ^{117}Sn could be a three-quasiparticle state involving large-j orbits. A candidate for the high-lying and high-spin state may be a $[(h_{\frac{11}{2}})^2\ 10^+,\ d_{\frac{3}{2}}]_{23/2^+}$ state, in which the third quasiparticle is coupled stretchwise with the $(h_{\frac{11}{2}})^2\ 10^+$ state appearing in the even isotopes. Of the multiplet of the $[(h_{\frac{11}{2}})^2\ 10^+,\ d_{\frac{3}{2}}]J$ configuration, the stretched state of $J = \frac{23}{2}$ is expected to be the lowest-lying if the $S = 0$ coupling of like particles is energetically favoured. The general feature of coupling schemes resulting in isomeric states is discussed elsewhere by Yamazaki [49]). A more detailed experimental study is required to establish the properties of this isomer in ^{117}Sn. Perhaps similar states might also be observed in other odd Sn isotopes with $N \geqq 67$.

5. Concluding remarks

We emphasize the possible presence of $(h_{\frac{11}{2}})^2\ 10^+ \rightarrow (h_{\frac{11}{2}})^2\ 8^+$ isomers in the region $N \geqq 64$, which preserve pure quasiparticle states. In the region $N < 64$, such an isomer is not observed, and the ground band terminates at a spin of 6^+. The discontinuance of the ground band structure in the region $N < 64$ is also seen in the $Z = 52$ Te isotopes studied by Bergström *et al.* [50]). These facts raise a question as to the real nature of the ground band of levels and the relation between the so-called vibrational sequence and the lowest-seniority scheme.

It should be noted that the present study was a survey of energy levels and isomeric states. There remain many experimental ambiguities which require detailed investigation. Of particular importance is the observation of the low-energy isomeric transitions themselves, which were outside the range of this survey.

The authors are grateful to Dr. S. G. Prussin for cooperation during the experiments, to Drs. J. M. Hollander and B. G. Harvey for support of this experimental program at the 2.2 m cyclotron at Berkeley and to F. S. Goulding and D. Landis for help with the electronic equipment required for these experiments. They would also like to thank Professors B. R. Mottelson and T. Udagawa for stimulating discussions and Professors I. Perlman and J. O. Rasmussen for the hospitality of the Lawrence Radiation Laboratory.

References

1) R M. Diamond and F. S. Stephens, Nucl Phys **45** (1963) 632
2) J. Burde, R. M. Diamond and F. S Stephens, Nucl. Phys. **85** (1966) 481
3) K. Brandi, R Engelmann, V. Hepp, E Kluge, H. Krehbiel and U. Meyer-Berkhout, Nucl Phys. **59** (1964) 33
4) A. L. McCarthy, B. L. Cohen and L. H Goldman, Phys. Rev **137B** (1965) 250
5) E. A. Ivanov, Phys. Lett **23** (1966) 265
6) A. L. McCarthy and T. W. Conlon, Phys. Rev. **147** (1966) 881
7) T W Conlon, Nucl Phys. **A100** (1967) 545
8) S. Bjørnholm, J Borggreen, H J. Frahm and N. J. S Hansen, Nucl. Phys **73** (1965) 593
9) T. Yamazaki and G. T Ewan, Phys Lett. **24B** (1967) 278

10) T. Yamazaki and G T. Ewan, Nucl. Instr. **62** (1968) 101
11) T Yamazaki, Proc. 1967 Enrico Fermi Int School of Physics at Varenna, Course XL (Academic Press, New York, to be published)
12) T. Yamazaki, E. Matthias, S. G. Prussin, C. M Lederer, J. M Jaklevic and J. M. Hollander, Contribution to Int. Conf. on nuclear structure, Tokyo (September 1967)
13) T. Yamazaki, G. T. Ewan and S. G Prussin, Phys Rev. Lett. **20** (1968) 1376
14) H. H Bolotin, A. C Li and A Schwarzschild, Phys Rev. **124** (1961) 213
15) H Ikegami and T Udagawa, Phys. Rev **124** (1961) 1518
16) H. H Bolotin, Phys. Rev. **136** (1964) B1557, B1566
17) E. Bodenstedt *et al.*, Nucl. Phys. **89** (1966) 305
18) M G Betigeri and H Morinaga, Nucl. Phys. **A95** (1967) 176
19) Ch Chang, G B. Hageman and T. Yamazaki, Nucl. Phys. **A134** (1969) 110
20) S D. Bloom, in Nuclear reactions, Vol. II, ed by P. M. Endt and P B. Smith (North-Holland Publ. Co , Amsterdam, 1962) p 1
21) G T Ewan, R. L Graham and I. K. McKenzie, IEEE Trans Nucl. Sci **NS-13** (1966) 297
22) J Pigneret, J. J Samuell and A. Sarazin, IEEE Trans. Nucl. Sci. **NS-13** (1966) 306
23) M. G. Strauss, R. N Larsen and L L. Sifter, IEEE Trans. Nucl. Sci. **NS-13** (1966) 265
24) S Gorni, G. Hochner, E. Nadav and H Zmora, Nucl. Instr **53** (1967) 349
25) H. G Jackson, Nucl Instr. **33** (1965) 161
26) C. M. P. Johnson, Phil. Mag. **1** (1956) 573
27) R Barloutaud, P Lehmann, A Leveque, G. C. Phillips and J Quidort, Compt Rend. **245** (1957) 422
28) K W Allen, D. Eccleshall and M. J. L. Yates, Proc. Phys. Soc. **74** (1959) 660
29) J A Becker, J. W. Olness and D. H. Wilkinson, Phys. Rev. **155** (1967) 1089
30) D C. Camp, Nucl. Phys. **A121** (1968) 561
31) E. Eichler, P. H. Stelson and J. K. Dickens, Phys. Lett., to be published
32) W D. Myers and W. J. Swiatecki, UCRL-11980 (May, 1965)
33) S. Fukushima, S. Hayashi, S. Kume, H Okamura, K. Otozai, K. Sakamoto and Y. Yoshizawa, Nucl Phys. **41** (1963) 275
34) S. Fukushima, S. Kume, H. Okamura, K. Otozai, K Sakamoto,Y. Yoshizawa and S. Hayashi, Nucl. Phys. **69** (1965) 273
35) C M. Lederer, J. M. Hollander and I. Perlman, Table of isotopes, 6th ed. (John Wiley and Sons, New York, 1967)
36) O Hansen and O. Nathan, Nucl. Phys **42** (1963) 197
37) M. Sakai, T Yamazaki and H Ejiri, Nucl. Phys. **74** (1965) 81
38) K. F Alexander, H F. Brinckmann, C. Heiser, G. Lang, W. Neubert and H. Rotter, Phys Lett. **17** (1965) 322
39) E. Ivanov, A Alevra, D Plostinaru, N. Martalogu and R. Dumitresu, Nucl. Phys. **54** (1964) 177
40) E. A. Ivanov and M. I. Magda, Rev. Roum. Phys. **12** (1967) 227
41) E. J Schneid, A. Prakash and B. L Cohen, Phys Rev. **156** (1967) 1316
42) L. S. Kisslinger and R. A. Sorensen, Mat. Fys Medd. Dan. Vid. Selsk. **32**, No. 9 (1960)
43) R. Arvieu, E. Baranger, M. Veneroni, M. Baranger and V. Gillet, Phys. Lett **4** (1963) 119
44) R Arvieu, Ann. de Phys. **8** (1963) 407
45) A. Plastino, R. Arvieu and S. A. Moszkowski, Phys. Rev. **145** (1966) 837
46) P. L. Ottaviani, M. Savoia, J. Sawicki and A. Tomasini, Phys. Rev. **153** (1967) 1138
47) R. L. Ottaviani, M Savoia and J Sawicki, Nuovo Cim. **56B** (1968) 149
48) M. Gmitro and J. Sawicki, Phys. Lett. **26B** (1968) 493;
M. Gmitro, A. Rimini, J. Sawicki and T Weber, Phys. Rev Lett **20** (1968) 1185
49) T Yamazaki, to be published
50) I Bergstrom, C. J. Herrlander, A Kerek and A Lukko, Contribution Int. Conf on nuclear structure, Tokyo, Japan (September 1967)